International Journal of Biochemistry and Cell Biology 114 (2019) 105564

Contents lists available at ScienceDirect

International Journal of Biochemistry and Cell Biology

journal homepage: www.elsevier.com/locate/biocel

Exosomes from adipose-derived mesenchymal stem cells ameliorate cardiac damage after myocardial infarction by activating S1P/SK1/S1PR1 signaling and promoting macrophage M2 polarization

Shengqiong Deng[a,1], Xianjin zhou[b,1], Zhiru Ge[c,1], Yuting Song[d,e], Hairong Wang[c], Xinghui Liu[a,*], Denghai Zhang[e,*]

[a] Department of Clinical Laboratory, Shanghai Gongli Hospital, The Second Military Medical University, Shanghai, 200135, China
[b] Shanghai First Maternity and Infant Hospital, Tongji University School of Medicine, Shanghai, 200135, China
[c] Department of Cardiology, Shanghai Gongli Hospital, The Second Military Medical University, Shanghai, 200135, China
[d] Ningxia Medical University, Ningxia, 750000, China
[e] Sino-French Cooperative Central Lab, Shanghai Gongli Hospital, Secondary Military Medical University, Shanghai, 200135, China

ARTICLE INFO

Keywords:
ADSCs
Sphingosine 1-phosphate
Macrophage
Exosome
Myocardial infarction

ABSTRACT

Exosomes derived from mesenchymal stem cells (MSCs) are known to participate in myocardial repair after myocardial infarction (MI), but the mechanism remains unclear. Here, we isolated exosomes from adipose-derived MSCs (ADSCs) and examined their effect on MI-induced cardiac damage. To examine the underlying mechanism, H9c2 cells, cardiac fibroblasts, and HAPI cells were used to study the effect of ADSC-exosomes on hypoxia-induced H9c2 apoptosis, TGF-β1-induced fibrosis of cardiac fibroblasts, and hypoxia-induced macrophage M1 polarization using qRT-PCR, western blot, ELISA, immunohistochemistry, immunofluorescence and flow cytometry. ADSC-exosome treatment mitigated MI-induced cardiac damage by suppressing cardiac dysfunction, cardiac apoptosis, cardiac fibrosis, and inflammatory responses in vitro and in vivo. In addition, ADSC-exosome treatment promoted macrophage M2 polarization. Further experiments found that S1P/SK1/S1PR1 signaling was involved in the ADSC-exosome-mediated myocardial repair. Silencing of S1PR1 reversed the inhibitory effect of ADSC-exosomes on MI-induced cardiac apoptosis and fibrosis in vitro. ADSC-exosome-induced macrophage M2 polarization was also reversed after downregulation of S1PR1 under hypoxia conditions, which promoted NFκB and TGF-β1 expression, and suppressed the MI-induced cardiac fibrosis and inflammatory response. In sum, these results indicate that ADSC-derived exosomes ameliorate cardiac damage after MI by activating S1P/SK1/S1PR1 signaling and promoting macrophage M2 polarization.

1. Introduction

Myocardial infarction (MI) is the main cause of mortality among cardiovascular diseases (Benjamin et al., 2017). Unlike other organs, a heart damaged by MI cannot repair itself through cardiac muscle cell regeneration (Wu et al., 2017). Instead, a fibrous scar replaces the necrotic myocardium, which leads to cardiac dysfunction and left ventricular remodeling (Dai et al., 2015). Exosome secretion from adipose-derived mesenchymal stem cells (ADSCs) is a safe and effective measure to prevent hypoxic ischemia-induced myocardial fibrosis and apoptosis (Liu et al., 2018a; Luo et al., 2017; Ma et al., 2017). However, the underlying mechanism remains largely unclear.

Exosomes are tiny membrane-bound vesicles (30˜100 nm) of endocytic origin that arise from the luminal membrane of multivesicular bodies and are actively secreted by a wide variety of cells. They are released constitutively by the fusion of multivesicular bodies with the cell membrane (Sahoo and Losordo, 2014). Exosomes can mediate organ-, tissue-, and cellular-level microcommunication under pathological and normal conditions by shuttling mRNA, proteins and microRNAs (miRNAs) (Gallet et al., 2017; Luther et al., 2018; Singla, 2016; Yuan et al., 2016).

Previous studies have shown that exosomes can regulate the polarization of macrophages. Macrophages can differentiate into the classical proinflammatory M1 phenotype or an anti-inflammatory M2

* Corresponding authors at: Shanghai Gongli Hospital, Second Military Medical University, 219 Miao-Pu Road, Shanghai, 200135, China.
E-mail addresses: joan0626@126.com (S. Deng), 8294461@qq.com (X. zhou), zhiruge@163.com (Z. Ge), WLJS816@qq.com (Y. Song), hairong19@yahoo.com (H. Wang), syliuxh@163.com (X. Liu), shanghai_zhang@hotmail.com (D. Zhang).
[1] These authors are co-First-Author.

https://doi.org/10.1016/j.biocel.2019.105564
Received 3 May 2019; Received in revised form 28 June 2019; Accepted 1 July 2019
Available online 02 July 2019

phenotype upon extracellular signaling from cytokines and molecules within the tumor microenvironment (Sica and Mantovani, 2012). miR-30d-5p-ADSCs exosomes reversed the changes caused by autophagy-mediated, acute ischemic stroke-induced brain injury through promotion of M2 macrophage/microglial polarization (Jiang et al., 2018). Exosomes derived from glioblastoma stem cells induce PD-L1 expression and M2 macrophage polarization in human monocytes (Gabrusiewicz et al., 2018). We therefore speculated that exosomes from ADSCs have cardioprotective effects related to macrophage polarization.

Activation of the sphingosine 1-phosphate (S1P), sphingosine kinase 1 (SphK1 or SK1), and sphingosine-1-phosphate receptor 1 (S1PR1) axis is crucial in various cellular signaling cascades and a number of pathological processes. In particular, the function of these molecules has been broadly investigated in cancer development/progression, immune function and angiogenesis, as well as inflammatory responses (Karliner, 2009). A recent study showed that the S1P/SK1/S1PR1 signal has important functions in cardiovascular disease (Cannavo et al., 2017). A study in melanoma found that downregulation of SK1 induces protective tumor immunity through the promotion of M1 macrophage responses (Mrad et al., 2016), suggesting that S1P/SK1/S1PR1 signaling has an important regulatory function in macrophage polarization. In this study, we studied the therapeutic effects of ADSC-exosomes on MI using MI rats and explored the underlying protective mechanism.

2. Materials & methods

2.1. Ethics statement

Male Sprague-Dawley rats (n = 18) aged eight weeks were purchased from SLAC Laboratory Animal Co. Ltd, Shanghai, China, and were individually fed in independent, ventilated cages at 24–26 °C and constant humidity in a 12 h light/dark cycle. The Pudong New Area Gongli Hospital Animal Ethics Committee, Shanghai, China approved the animal experiments.

2.2. ADSCs isolation, culture and identification

Briefly, adipose tissue was harvested from normal rats, washed with phosphate-buffered saline (PBS), and minced before digestion with 0.2% collagenase I (Sigma-Aldrich, St. Louis, MO, USA) for 1 h at 37 °C with intermittent shaking. The digested tissue was washed with Dulbecco's modified Eagle's medium (DMEM, Sigma-Aldrich) containing 15% FBS (Gibco BRL, Maryland, USA) and was then centrifuged at 1200 *g* for 10 min to remove mature adipocytes. We resuspended the pellet in DMEM supplemented with 15% FBS, 100 U/ml penicillin, and 100 μg/ml streptomycin followed by culture at 37 °C and 5% CO_2. ADSCs reaching 80%–90% confluence were detached with multiple incubations of 0.02% ethylenediaminetetraacetic acid (EDTA)/0.25% trypsin (Sigma-Aldrich) for 5 min at room temperature, as needed. Fluorescein isothiocyanate (FITC)- or phycoerythrin (PE)-conjugated CD90, CD29, CD105, CD44, CD34, and von Willebrand Factor (vWF) antibodies were used for phenotypic analysis. An IgG-matched isotype was utilized as the internal antibody control. Normoxic ADSC cultures were grown in 95% air containing 20% O_2 and 5% CO_2.

2.3. ADSC multilineage differentiation

To evaluate multilineage differentiation of ADSCs, third-passage rat ADSCs were cultivated in adipogenic differentiation medium and stained using oil-**red**-O after fourteen days, or cultivated in osteogenic differentiation medium and stained with alizarin red after twenty-one days.

2.4. ADSC-derived exosome identification and isolation

After reaching 80–90% confluence, the ADSCs were rinsed with PBS and cultivated in FBS-free endothelial cell growth medium (EGM)-2 MV supplied with 1 × serum replacement solution (PeproTech, New Jersey, USA) for another 48 h. The conditioned culture medium (100 ml conditioned culture medium from 1×10^8 cells) was removed and centrifuged at 300 *g* for 10 min and then at 10,000 *g* for 10 min to remove cellular debris and dead cells. Then, exosomes were pelleted by ultracentrifugation at 100,000 *g* for 70 min and washed once using PBS. Exosomes were pelleted once again by ultracentrifugation at 100,000 *g* for an additional 70 min. We resuspended the exosome pellet in PBS for the subsequent tests. We quantified exosome numbers using a Zetasizer Nano (Malvern Instruments, Malvern, UK) and assessed the purity through western blotting with exosome markers (CD63, CD81, and CD9) and transmission electron microscopy.

2.5. Myocardial infarction model

We induced MI through the left anterior descending coronary artery (LAD) by surgical ligation. Animals were anesthetized using diazepam (5 mg/kg) and ketamine hydrochloride (50 mg/kg). Then, we opened the left fourth intercostal space chest and ligated the LAD with a 6-0 silk suture 1 mm below the left atrial appendage tip. Satisfactory ligation was confirmed by the color change. After 1 h of ligation, rats received saline injection or ADSC-derived exosomes (2.5×10^{12} particles suspended in 500 μL PBS) through the inferior vena cava. The control group received left thoracotomy without ligation as a sham-operated group. We closed the chest with 4–0 sutures. The rats were kept for 1 month before echocardiography assessment and histology studies. Each group comprised 6 rats.

2.6. Echocardiographic and hemodynamic measurements

We anesthetized rats with intramuscular injections of ketamine (100 mg/kg) and medetomidine (0.25 mg/kg). Cardiac function parameters such as left ventricular internal dimension in systole (LVID(s)), left ventricular internal dimension in diastole (LVID(d)), left ventricular fraction shortening (LVFS), and left ventricular ejection fraction (LVEF) were captured by a transthoracic echocardiography system, which had a 15 MHz phased-array transducer (SONOS 5500, Hewlett-Packard, Andover, USA).

We inserted a catheter into the rat left ventricle from the right carotid artery. In this manner, the left ventricular end diastolic pressure (LVEDP), heart rate (HR), and cardiac contractility (dP/dt maximum and dP/dt minimum) were assayed and recorded with a PowerLab ML880 (AD Instrument, Australia).

2.7. Immunofluorescence and immunohistochemistry analysis

Myocardial tissue samples from infarction area were fixed in 10% formalin solution, embedded in paraffin, and sectioned at 5 μm. The tissue sections were stained with Masson's trichrome for histological evaluation. Immunofluorescence staining for F4/80, CD11b, and CD206 was performed to evaluate macrophage polarization, and the results were analyzed by Axiophot light microscope (Zeiss, Oberkochen, Germany) and fluorescence microscope (Nikon, Tokyo, Japan), which were photographed with a digital camera.

2.8. Cell culture and induction

Rat-derived H9c2 cells were purchased from the American Type Culture Collection (ATCC, Rockville, USA). We cultivated cells in DMEM high-glucose medium (Hyclone, Logan, UT, USA) containing 10% FBS (Hyclone), 100 μg/ml streptomycin, and 100 U/ml penicillin at 37 °C in a humidified incubator with an atmosphere of 5% CO_2. The

Table 1
Primer sequences for RT-PCR.

Gene	Forward Primer	Reverse Primer
IL-1β	5′-CCTCGTCCTAAGTCACTCGC-3′	5′-GCAGAGTCTTTTTGACCCTCCT-3′
IL-6	5′-CCAGTTGCCTTCTTGGGACT-3′	5′-TCTGACAGTGCATCATCGCT-3′
TGF-β1	5̇-TGCGCCTGCAGAGATTCAAG-3′	5′-AGGTAACGCCAGGAATTGTTGCTA-3′
TNF-α	5̇-CTCTTCTCATTCCCGCTCGT-3′	5̇-GGGAGCCCATTTGGGAACTT-3′
IFN-γ	5̇-TTCGAGGTGAACAACCCACA-3′	5̇-CACTCTCTACCCCAGAATCAGC-3′
Arg1	5̇-TCACCTGAGCTTTGATGTCG-3′	5̇-TTCCCAAGAGTTGGGTTCAC-3′
Ym1	5̇-ACCCCTGCCTGTGTACTCACCT-3′	5̇-CACTGAACGGGGCAGGTCCAAA-3′
IL-10	5̇-TGATGCCCCAAGCTGAGAAC-3′	5̇-AATCGATGACAGCGCCGTAG-3′
GAPDH	5̇-TGCCACTCA GAAGACTGTGG-3′	5̇-TTCAGCTCTGGGATGACCTT-3′

culture medium was replaced every two days. For hypoxia induction, H9c2 cells were cultured in 93% N_2, 2% O_2, and 5% CO_2 with or without polydatin treatment (100 μM).

To analyze myocardial fibrosis, we isolated cardiac fibroblasts by enzymatic digestion with trypsin and collagenase, as previously described (Ohkura et al., 2017). In brief, we dissected and isolated hearts free of atria and vessels. We inserted a cannula into the ascending aorta and perfused the hearts for 4 min with collagenase buffer containing 0.3% (wt/vol) collagenase type II (Worthington) and 0.05% trypsin (Worthington) in Krebs buffer at 37 °C. We finely fragmented the digested heart tissues using gentle pipetting and filtered them through a mesh (BD Biosciences). Cell suspensions were centrifuged at 400 *g* and resuspended in DMEM containing 10% fetal bovine serum. We plated the suspended cells and collected non-adherent cells 1 h later. Adherent cardiac fibroblasts were expanded by dispersal with trypsin/EDTA solution after reaching confluence followed by replating at a 1:4 split rate. We visually confirmed the characteristic fibroblast morphology using a light microscope. Almost 100% of the cells were positive for anti-vimentin staining. Because fibroblast phenotypes can be affected by growth conditions such as passage number, fibroblasts were utilized at passage 1–3 for our experiments. To analyze myocardial fibrosis, fibroblasts were pretreated with/without ADSCs-exosomes (200 μg/ml) before induction with TGF-β1 (100 μg/mL) for 24 h.

HAPI cells were purchased from Procell (Wuhan, China) for microglia/macrophage polarization analysis. We cultivated the cells in DMEM high-glucose medium (Hyclone), containing 10% FBS (Hyclone), 100 μg/ml streptomycin, and 100 U/ml penicillin at 37 °C in a humidified incubator with an atmosphere containing 5% CO_2. We replaced the culture medium every 2 days. To study the effect of ADSC-exosomes on macrophage polarization, HAPI cells were pretreated with/without ADSC-exosomes (200 μg/ml) before exposure to hypoxia conditions.

2.9. Western blot assay

Cells or tissues were lysed centrifuged at 12,000 rpm at 4 °C following the addition of a protease inhibitor. Protein concentration was determined with a Pierce bicinchoninic acid assay (BCA) kit (Thermo Fisher). We separated proteins using 10% SDS-PAGE and transferred them to PVDF membranes. The primary antibodies used to assay protein expression were CD81 (1:600), CD63 (1:600), CD9 (1:600), SK1 (1:1000), S1PR1 (1:500), NF-κB p65 (1:600), TGF-β1 (1:200), α-SMA (1:500, all from Santa Cruz Biotechnology, Dallas, USA), collagen III (1:500), collagen I (1:500), and anti-GAPDH (1:1000, Sigma-Aldrich). Horseradish peroxidase-conjugated secondary antibodies (1:1000, Abcam, USA) were used. An ECL chemiluminescence kit (Millipore, Burlington, MA, USA) was used to read the bands.

2.10. Flow cytometry

We employed flow cytometry to assay H9c2 cell apoptosis with FITC-conjugated annexin V (AV) and propidium iodide (PI) staining. Cells were washed twice and adjusted to 1×10^6 cells/ml in cold D-Hanks buffer. PI (10 μl) and AV-FITC (10 μl) were added to 100 μL of cell suspension, which was then incubated for 15 min at room temperature in the dark. Prior to analysis, 400 μl binding buffer was added to each sample without processing. Each assay was performed at least in triplicate.

2.11. RNA interference

The siRNA vector against S1PR1 (siS1PR1) was purchased from RiboBio (Guangzhou, China), and transfection was performed following the supplier's protocol. Briefly, H9c2 cells, HAPI microglia cells, or fibroblasts were transfected with either siS1PR1 or negative control (NC) at a final concentration of 50 nM using Lipofectamine® 2000 (Sigma-Aldrich) following the standard procedure. Analysis of S1PR1 expression or subsequent experiments were performed after 48 h of transfection.

2.12. Real-time RT-PCR

We isolated RNA using TRIzol reagent (Invitrogen, Carlsbad, USA), the RNA quantification was done by Nanodrop (Thermo Scientific, Rockford, IL, USA) and cDNA was synthesized using Improm II reverse transcription kit (Promega, Madison, WI, USA) following the manufacturer's instructions. RT-PCR was performed with SYBR Green to detect mRNA levels, which were quantified by the $2^{-\Delta\Delta Ct}$ method. The primers for target genes (Table 1) were obtained from GenePharma (Shanghai, China).

2.13. Enzyme-linked immunosorbent assay (ELISA)

We collected cell culture medium after the indicated treatments. ELISA kits (R&D Systems) were used to determine the levels of interleukin (IL)-6, IL-1β, interferon (IFN)-γ, and tumor necrosis factor (TNF)-α, following the standard instructions. We measured S1P concentrations with the sphingosine-1-phosphate enzyme-linked immunosorbent assay kit (K-1900; Echelon, Beijing, China) following the standard process.

2.14. Statistics analyses

Continuous variables were denoted as the mean ± standard deviation (SD). We used one-way analysis of variance for multiple comparisons using GraphPad software package (GraphPad, La Jolla, USA). A P-value ≤ 0.05 was considered statistically significant.

3. Results

3.1. ADSC-exosome characterization

Previous studies reported that ADSCs-derived exosomes have a protective effect by attenuating MI-induced myocardial damage (Liu

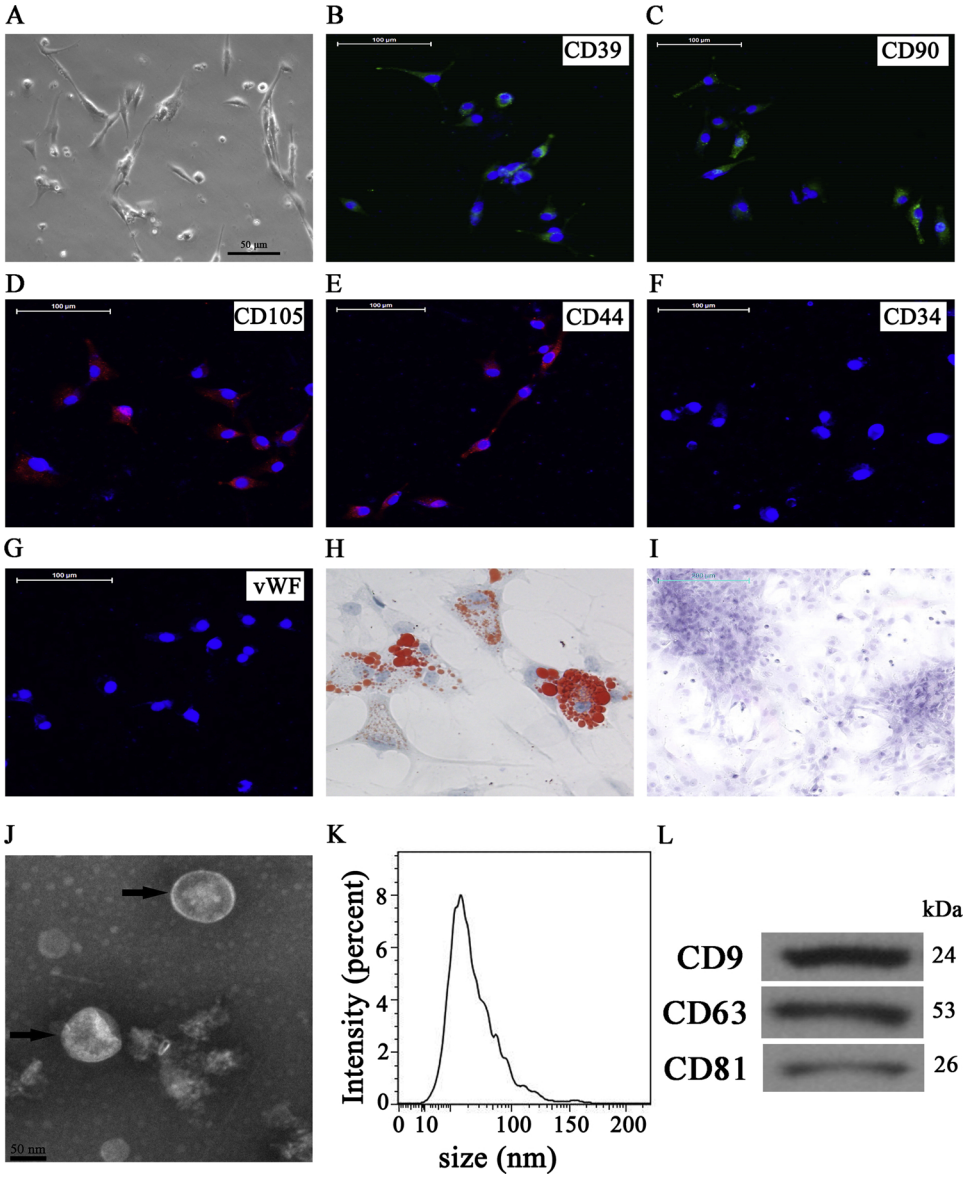

Fig. 1. Characterization of adipose-derived stem cells (ADSCs) and ADSC-derived exosomes. (A) ADSCs showed a typical cobblestone-like morphology. (B–G) Immunofluorescence staining of cell surface markers. The antibodies were labeled with either fluorescein isothiocyanate (FITC, green) or phycoerythrin (PE, red). CD29, CD90, CD44, and CD105 are positive. CD34 and von Willebrand Factor (vWF) are negative. (H and I) Differentiation potential of ADSCs assessed by oil-red-O (H) and alkaline phosphatase staining (I). (J) Transmission electron micrographs showing ADSC-exosome morphology. (K) Particle size of ADSC-exosomes was measured by Zetasizer Nano. (L) Western blots of CD9, CD63, and CD81 expression in exosomes from ADSCs (For interpretation of the references to colour in this figure legend, the reader is referred to the web version of this article.).

et al., 2018a; Luo et al., 2017). However, the underlying mechanism remains unknown. In this study, we isolated ADSCs confirmed their typical cobblestone-like morphology (Fig. 1A). Immunofluorescence staining was positive for the expression of the mesenchymal cell markers CD44, CD105, CD29, and CD90 and negative for the endothelial markers vWF and CD34 (Fig. 1B–G). The oil-red-O and alizarin red staining results confirmed that ADSCs can differentiate into multiple lineages including adipocytes and osteoblasts (Fig. 1H and I).

Transmission electron micrograph detection showed that ADSC-exosomes exhibited the characteristic cup-shaped morphology (Fig. 1J). Exosomes size was quantified with a Zetasizer Nano. The mean vesicle diameter was 80–130 nm (Fig. 1K), which was consistent with previously described exosomes (Du et al., 2017). Western blot analysis of exosome lysates showed positive expression of the exosome proteins CD63, CD81, and CD9 (Fig. 1L). These data indicated that the nanoparticles were exosomes.

3.2. Effect of ADSC-derived exosomes to MI-induced myocardial injury and cardiac dysfunction

To examine the effect of ADSC-exosomes, rats were injected with ADSC-derived exosomes after 1 h of ligation. At 1 month after ligation, echocardiography showed significantly decreased LVFS and LVEF, while LVID significantly elevated in MI rats compared with sham rats; importantly, these changes were partially alleviated by exosome treatment. Hemodynamic examination demonstrated that MI decreased dP/dt and increased LVEDP, which were both ameliorated by exosome treatment (Table 2).

Pathological analysis showed a significantly higher rate of diffuse collagen fiber accumulation in both perivascular and interstitial areas in MI rats compared with sham operation rats. Exosome treatment significantly decreased MI-induced myocardial fibrosis (Fig. 2A and B). Immunohistochemical analysis showed that myocardial cell apoptosis in the infarction area was markedly elevated after MI, and exosome treatment significantly decreased MI-induced myocardial apoptosis (Fig. 2C and D). These data illustrated that ADSC-derived exosomes exert a protective effect on myocardial injury by reversing MI-induced myocardial fibrosis and apoptosis.

3.3. ADSC-derived exosomes attenuate MI-induced inflammation by promoting macrophage M2 polarization

Inflammatory factors in serum were detected by ELISA, and the results showed that treatment with ADSC-derived exosomes reduced

Table 2
Echocardiographic and hemodynamic parameters.

	Sham	MI	MI + Exosome
Echocardiography			
LVEF (%)	64 ± 2.63	36 ± 2.18***	48 ± 1.99###
LVFS (%)	35 ± 2.06	18 ± 2.18***	28 ± 2.31###
LVID(d) (mm)	6.92 ± 0.32	9.63 ± 0.24***	8.26 ± 0.41#
LVID(s) (mm)	3.42 ± 0.23	8.55 ± 0.28***	6.57 ± 0.46#
Hemodynamic			
HR (bpm)	391 ± 18	423 ± 16	409 ± 18
dP/dt max (mm Hg/s)	5588 ± 236	3678 ± 205***	4613 ± 188###
dP/dt min (mm Hg/s)	4029 ± 182	2615 ± 211***	3257 ± 198###
LVEDP (mmHg)	7.53 ± 0.56	14.26 ± 0.62***	9.32 ± 0.29###

LVEF, left ventricular ejection fraction; LVFS, left ventricular fraction shortening; LVID(d), left ventricular internal dimension in diastole; LVID(s), left ventricular internal dimension in systole; HR, heart rate; dP/dt max, maximal slope of systolic pressure increment; dP/dt min, minimal slope of diastolic pressure decrement; LVEDP, left ventricular end-diastolic pressure. Data are means ± SEM. *P < 0.05 versus the sham group.
# P < 0.05.
P < 0.001 versus the MI group.
*** P < 0.001.

the amount of MI-induced IL-6, IL-1β, IFN-γ and TNF-α (Fig. 3A–D). An increasing number of studies have demonstrated that macrophage polarization participates in inflammatory responses (Han et al., 2018; Sieve et al., 2018). In our study, we found that MI upregulated the expression of M1 macrophage markers IL-1β, IL-6, TNF-α, and IFN-γ, whereas it have no effect to M2 macrophage markers Arg1, Ym1, TGF-β1, and IL-10 expression (Fig. 3E–L). This suggested that MI promoted macrophage differentiation towards the M1 phenotype. ADSC-derived exosome treatment reversed MI-induced M1 macrophage differentiation and promoted M2 macrophage differentiation. In addition, MI downregulated S1P, SK1, and S1PR1, whereas exosome treatment upregulated S1P, SK1, and S1PR1 expression (Fig. 3M–Q). These data indicated that the S1P/SK1/S1PR1 signaling pathway may participate in the cardioprotective and anti-inflammatory effects of ADSC-exosomes, and exosome treatment reversed MI-induced NF-κB p65 activation.

3.4. ADSC-derived exosome treatment decreases hypoxia-induced myocardial apoptosis and fibrosis by activating S1P/SK1/S1PR1 signaling

To confirm the involvement of S1P/SK1/S1PR1 signaling in the cardioprotective effect of ADSC-derived exosomes, H9c2 cells transfected with siRNA against S1PR1 (siS1PR1) or NC were pretreated with/without ADSC-exosomes (200 μg/ml) before exposure to hypoxia conditions for 24 h. Flow cytometry showed that H9c2 cell apoptosis was significantly increased after exposure to hypoxic conditions. Pretreatment with ADSC-derived exosomes decreased hypoxia-induced H9c2 cell apoptosis (Fig. 4). Silencing of S1PR1 reversed the protective effect of ADSC-derived exosomes on hypoxia-induced H9c2 cell apoptosis.

Rat cardiac fibroblasts transfected with siS1PR1 or NC were pretreated with/without ADSC-exosomes (200 μg/ml) before induction by TGF-β1 (100 μg/mL) for 24 h. Western blot detection confirmed that TGF-β1 significantly upregulated the expression of fibrosis-promoting proteins including collagen I, collagen III, and α-SMA, and treatment with ADSC-derived exosomes downregulated fibrotic protein expression. However, Silencing of S1PR1 rescued the expression of fibrotic proteins even after pretreatment with ADSC-derived exosomes (Fig. 5).

Taken together, these data suggested that the S1P/SK1/S1PR1 signaling pathway participated in the cardioprotective effects ADSC-exosomes.

3.5. ADSC-derived exosome treatment decreases LPS-induced inflammation by activating S1P/SK1/S1PR1 signaling

To confirm the involvement of S1P/SK1/S1PR1 signaling in the regulation of macrophage polarization, rat HAPI microglia cells transfected with siS1PR1 or NC were pretreated with/without ADSC-

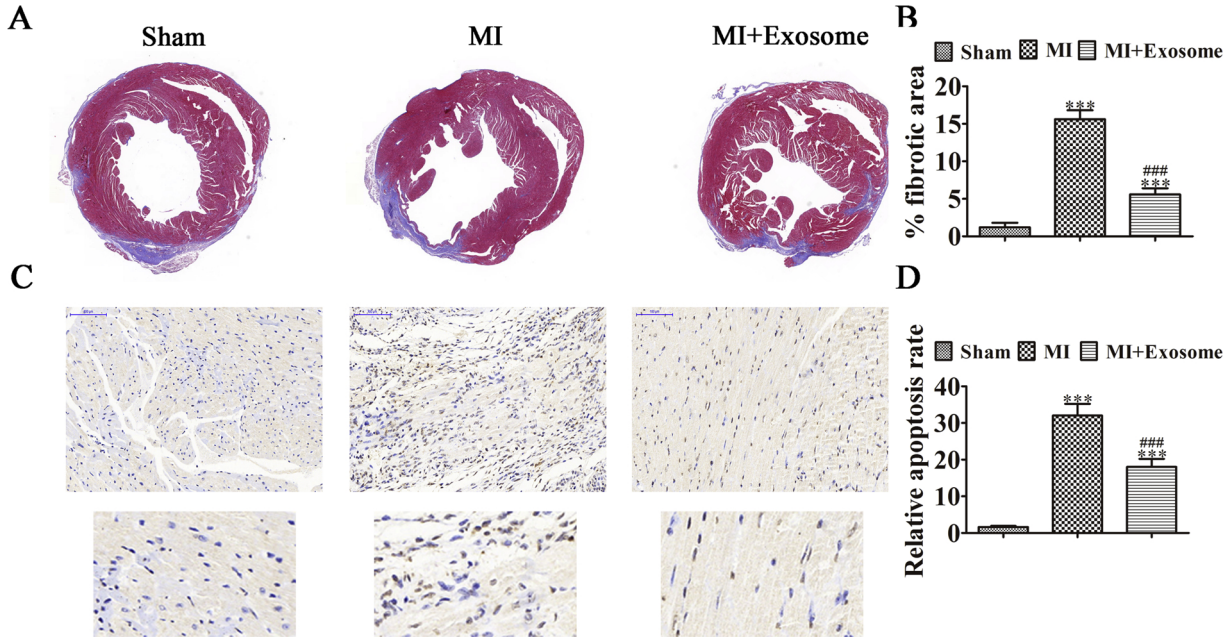

Fig. 2. Protective effect of ADSC-derived exosomes on myocardial injury after myocardial infarction (MI). (A and B) Masson's trichrome staining showing myocardial fibrosis according to collagen deposition (blue). Relative infarction size and tissue fibrosis were analyzed. Data are presented as the mean ± SEM. ***p < 0.001 versus Sham group. ###p < 0.001 versus MI group. (C and D) Immunohistochemical detection of apoptosis of myocardial cells in the infarction area using TUNEL (terminal deoxynucleotidyl-transferase-mediated dUTP nick-end labelling) staining. Relative infarction size and tissue fibrosis were analyzed. Data are presented as the mean ± SEM. ***p < 0.001 versus Sham group. ###p < 0.001 versus MI group (For interpretation of the references to colour in this figure legend, the reader is referred to the web version of this article.).

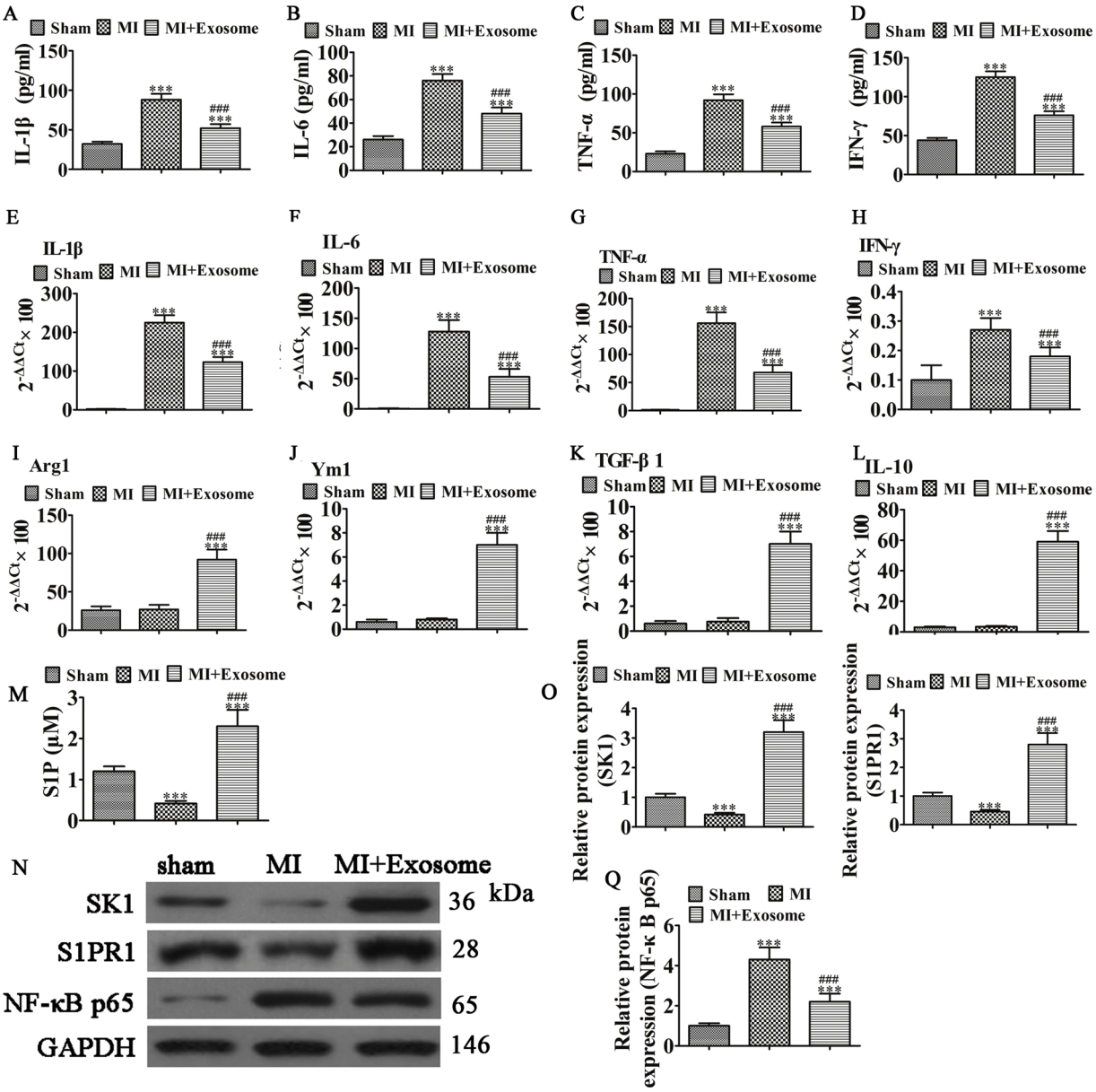

Fig. 3. ADSC-derived exosome treatment decreased MI-induced inflammation by promoting macrophage M2 polarization. (A–D) ELISA analysis showing the expression of inflammatory factors IL-1β, IL-6, TNF-α, and IFN-γ. Data are presented as the mean ± SEM. $^{***}p < 0.001$ versus Sham group. $^{\#\#\#}p < 0.001$ versus MI group. (E–L) qRt-PCR detection of the expression of M1 macrophage markers [IL-1β (E), IL-6 (F), TNF-α (G), and IFN-γ (H)] and M2 macrophage markers [Arg1 (I), Ym1 (J), TGF-β1 (K), and IL-10 (L)]. Data are presented as the mean ± SEM. $^{***}p < 0.001$ versus Sham group. $^{\#\#\#}p < 0.001$ versus MI group. (M) The expression of sphingosine 1-phosphate (S1P) in serum were detected by ELISA. Data are presented as the mean ± SEM. $^{***}p < 0.001$ versus Sham group. $^{\#\#\#}p < 0.001$ versus MI group. (N–Q) Western blot detection of the expression of sphingosine kinase 1 (SK1), sphingosine 1-phosphate receptor 1 (S1PR1), and NF-κB p65. Data are presented as the mean ± SEM. $^{***}p < 0.001$ versus Sham group. $^{\#\#\#}p < 0.001$ versus MI group.

exosomes (200 μg/ml) before exposure to hypoxia conditions. Immunofluorescence analysis showed that ADSC-exosome treatment upregulated CD206 (M2 macrophage marker) expression and downregulated hypoxia-induced CD11b (M1 macrophage marker) expression. Silencing of S1PR1 downregulated CD206 expression even after pretreatment with ADSC-derived exosomes (Fig. 6A–C). The ELISA results showed that S1PR1 downregulation reversed the anti-inflammatory effect of ADSC-exosomes (Fig. 6D–G). Western blot and ELISA assays showed that ADSC-exosomes activated S1P/SK1/S1PR1 signaling and downregulated NF-κB p65 and TGF-β1 expression in macrophages (Fig. 6H–M). These results suggested that ADSC-exosome treatment promoted macrophage M2 polarization, which inhibited inflammatory responses and attenuated myocardial fibrosis by suppressing NF-κB p65 and TGF-β1 expression.

4. Discussion

In the present research, we successfully characterized and isolated exosomes from ADSCs. The results showed that ADSC-exosome treatment significantly improved cardiac function as determined by echocardiographic and hemodynamic measurements. Pathological examination showed that ADSC-exosome treatment suppressed MI-induced myocardial fibrosis and apoptosis, as reported previously (Khan et al., 2015; Yamaguchi et al., 2015). ADSC-exosome treatment downregulated MI-induced inflammatory factor expression. Further investigation to determine whether macrophages were involved in the MI-induced inflammatory response showed that ADSC-exosome treatment promoted macrophage M2 polarization. Studies have shown that alternatively activated M2 macrophages exert anti-inflammatory effects

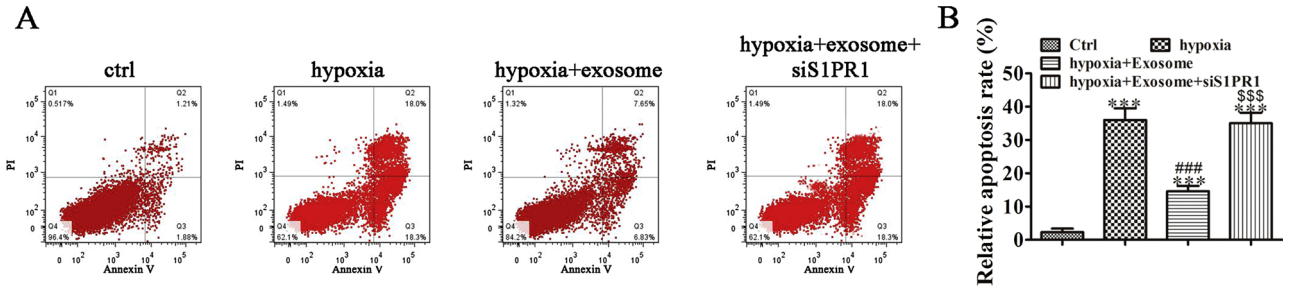

Fig. 4. ADSC-derived exosomes decreased hypoxia induced myocardial apoptosis by activating S1P/SK1/S1PR1 signaling. H9c2 cells transfected with siRNA against S1PR1 (siS1PR1) or negative control (NC) were pretreated with/without ADSC-exosomes (200 μg/ml) before exposure to the hypoxia condition for 24 h. (A) H9c2 apoptosis was assayed by flow cytometry after annexin V-FITC staining of cells cultured under the hypoxia condition for 24 h. (B) The apoptosis rate was determined at least five times. n = 5. Data are presented as the mean ± SEM. $^{***}p < 0.001$ versus ctrl group. $^{###}p < 0.001$ versus hypoxia group. $^{$$$}p < 0.001$ versus hypoxia + exosome group. Ctrl, control.

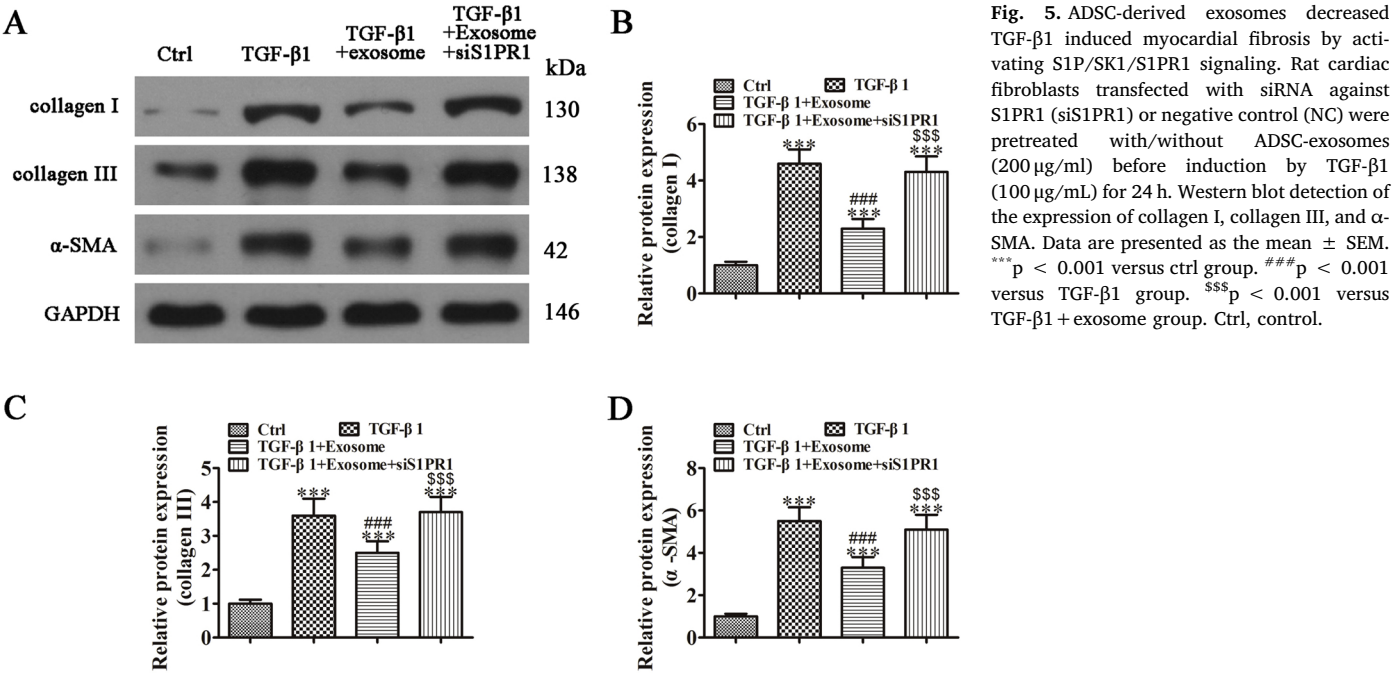

Fig. 5. ADSC-derived exosomes decreased TGF-β1 induced myocardial fibrosis by activating S1P/SK1/S1PR1 signaling. Rat cardiac fibroblasts transfected with siRNA against S1PR1 (siS1PR1) or negative control (NC) were pretreated with/without ADSC-exosomes (200 μg/ml) before induction by TGF-β1 (100 μg/mL) for 24 h. Western blot detection of the expression of collagen I, collagen III, and α-SMA. Data are presented as the mean ± SEM. $^{***}p < 0.001$ versus ctrl group. $^{###}p < 0.001$ versus TGF-β1 group. $^{$$$}p < 0.001$ versus TGF-β1 + exosome group. Ctrl, control.

(Kim et al., 2014; Kroner et al., 2014). In addition, we showed that ADSC-exosome treatment activated S1P/SK1/S1PR1 signaling.

To determine whether S1P/SK1/S1PR1 signaling was involved in ADSC-exosome-mediated myocardial protection, H9c2 cardiac fibroblasts and HAPI microglia cells were transfected with siRNA against S1PR1. Knockdown of S1PR1 reversed the suppressive effect of ADSC-exosomes on hypoxia-induced H9c2 apoptosis, TGF-β1-induced cardiac fibroblast fibrosis, and hypoxia-induced macrophage M1 polarization of HAPI microglia cells, suggesting that S1P/SK1/S1PR1 signaling is important in ADSC-exosome-mediated myocardial protection. Downregulation of S1PR1 suppressed ADSC-exosome-induced macrophage M2 polarization, leading to the upregulation of inflammatory factors. In addition, we verified the important function of NFκB in inflammatory factor expression. Silencing of S1PR1 promoted macrophage M1 polarization and upregulated NFκB (Islam et al., 2018).

In addition to the effect on inflammatory responses, TGF-β1 expression was also upregulated in M1 macrophages. TGF-β1 has an important role in cardiac fibroblast induction by regulating the TGF-β/Smad signaling pathway (Huang et al., 2018; Liu et al., 2018b; Shen et al., 2018). TGF-β1 inhibits S1PR1 expression (Chang et al., 2014); however, S1PR1 activation promotes macrophage M2 polarization, resulting in TGF-β1 inhibition. Suggestion that S1PR1 was the therapeutic target of ADSC-exosome-mediated myocardial protection. Increasing evidence have found that exosome have emerged as crucial mediators of intercellular communication. Exosome encapsulate and convey information to surrounding cells or distant cells, where they mediate cellular biological responses. Such as promoting angiogenesis in tissue regeneration (Saha et al., 2019; Shi et al., 2019). In this study we first found that ADSC-exosome-mediated myocardial protection relative to microenvironmental regulation. But the specific regulatory mechanisms underlying these phenomena require further study.

In conclusion, the results from the current study demonstrated that ADSC-derived exosomes ameliorate cardiac damage after MI by activating S1P/SK1/S1PR1 signaling and promoting macrophage M2 polarization.

Funding

This work was supported by the National Natural Science Foundation of China (grant 81700428); the Foundation of Discipline Leader in Health Systems of Pudong New District (grant PWRq2016-35); Discipline Construction Project of Pudong Health Bureau of Shanghai (Grant PWZxq-2017-15); Featured Special Disease Fund of Pudong New District (grant PWZzb2017-27); Postdoctoral fund of Shanghai Gongli Hospital of Secondary Military Medical University (GLBH2017002).

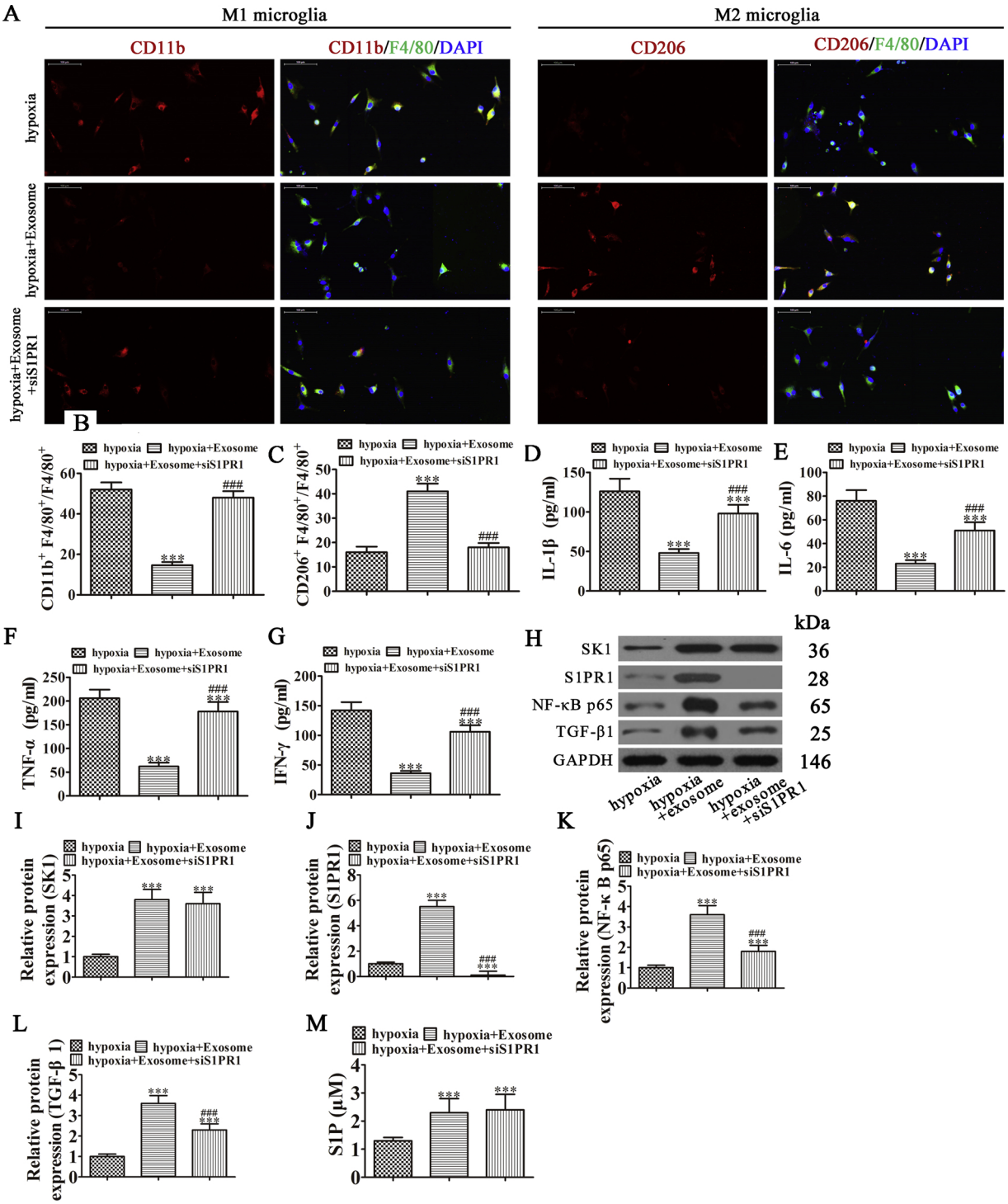

Fig. 6. ADSC-derived exosomes decreased LPS induced inflammation by activating S1P/SK1/S1PR1 signaling. Rat HAPI microglia cells transfected with siRNA against S1PR1 (siS1PR1) or negative control (NC) were pretreated with/without ADSC-exosomes (200 μg/ml) before exposure to the hypoxia condition. (A–C) Immunofluorescence detection of macrophage polarization by F4/80$^+$, CD11b$^+$ or CD206$^+$ staining. Data are presented as the mean ± SEM. $^{***}p < 0.001$ versus hypoxia group. $^{\#\#\#}p < 0.001$ versus hypoxia + exosome group. (D–G) ELISA analysis of the expression of inflammatory factors IL-1β, IL-6, TNF-α, and IFN-γ. (H–L) Western blot detection of the expression of SK1, S1PR1, NF-κB p65, and TGF-β1. Data are presented as the mean ± SEM. $^{***}p < 0.001$ versus hypoxia group. $^{\#\#\#}p < 0.001$ versus hypoxia + exosome group. (M) ELISA detection shows the expression of S1P. Data are presented as the mean ± SEM. $^{***}p < 0.001$ versus hypoxia group.

Ethical approval

The Pudong New Area Gongli Hospital Animal Ethics Committee, Shanghai, China approved all animal experiments.

References

Benjamin, E.J., Blaha, M.J., Chiuve, S.E., Cushman, M., Das, S.R., Deo, R., et al., 2017. Heart disease and stroke Statistics-2017 update: a report from the american heart association. Circulation 135, e146–e603.

Cannavo, A., Liccardo, D., Komici, K., Corbi, G., de Lucia, C., Femminella, G.D., et al., 2017. Sphingosine kinases and sphingosine 1-Phosphate receptors: signaling and actions in the cardiovascular system. Front. Pharmacol. 8, 556.

Chang, N., Xiu, L., Li, L., 2014. Sphingosine 1-phosphate receptors negatively regulate collagen type I/III expression in human bone marrow-derived mesenchymal stem cell. J. Cell. Biochem. 115, 359–367.

Dai, W., Herring, M.J., Hale, S.L., Kloner, R.A., 2015. Rapid surface cooling by ThermoSuit system dramatically reduces scar size, prevents post-infarction adverse left ventricular remodeling, and improves cardiac function in rats. J. Am. Heart Assoc. 4.

Du, Y., Li, D., Han, C., Wu, H., Xu, L., Zhang, M., et al., 2017. Exosomes from human-induced pluripotent stem cell-derived mesenchymal stromal cells (hiPSC-MSCs) protect liver against hepatic ischemia/ reperfusion injury via activating sphingosine kinase and Sphingosine-1-Phosphate signaling pathway. Cell. Physiol. Biochem. 43, 611–625.

Gabrusiewicz, K., Li, X., Wei, J., Hashimoto, Y., Marisetty, A.L., Ott, M., et al., 2018. Glioblastoma stem cell-derived exosomes induce M2 macrophages and PD-L1 expression on human monocytes. Oncoimmunology 7, e1412909.

Gallet, R., Dawkins, J., Valle, J., Simsolo, E., de Couto, G., Middleton, R., et al., 2017. Exosomes secreted by cardiosphere-derived cells reduce scarring, attenuate adverse remodelling, and improve function in acute and chronic porcine myocardial infarction. Eur. Heart J. 38, 201–211.

Han, J., Kim, Y.S., Lim, M.Y., Kim, H.Y., Kong, S., Kang, M., et al., 2018. Dual roles of graphene oxide to attenuate inflammation and elicit timely polarization of macrophage phenotypes for cardiac repair. ACS Nano 12, 1959–1977.

Huang, D.D., Huang, H.F., Yang, Q., Chen, X.Q., 2018. Liraglutide improves myocardial fibrosis after myocardial infarction through inhibition of CTGF by activating cAMP in mice. Eur. Rev. Med. Pharmacol. Sci. 22, 4648–4656.

Islam, S.U., Lee, J.H., Shehzad, A., Ahn, E.M., Lee, Y.M., Lee, Y.S., 2018. Decursinol angelate inhibits LPS-Induced macrophage polarization through modulation of the NFkappaB and MAPK signaling pathways. Molecules 23.

Jiang, M., Wang, H., Jin, M., Yang, X., Ji, H., Jiang, Y., et al., 2018. Exosomes from MiR-30d-5p-ADSCs Reverse Acute Ischemic Stroke-Induced, Autophagy-Mediated Brain Injury by Promoting M2 Microglial/Macrophage Polarization. Cell. Physiol. Biochem. 47, 864–878.

Karliner, J.S., 2009. Sphingosine kinase and sphingosine 1-phosphate in cardioprotection. J. Cardiovasc. Pharmacol. 53, 189–197.

Khan, M., Nickoloff, E., Abramova, T., Johnson, J., Verma, S.K., Krishnamurthy, P., et al., 2015. Embryonic stem cell-derived exosomes promote endogenous repair mechanisms and enhance cardiac function following myocardial infarction. Circ. Res. 117, 52–64.

Kim, Y.G., Udayanga, K.G., Totsuka, N., Weinberg, J.B., Nunez, G., Shibuya, A., 2014. Gut dysbiosis promotes M2 macrophage polarization and allergic airway inflammation via fungi-induced PGE(2). Cell Host Microbe 15, 95–102.

Kroner, A., Greenhalgh, A.D., Zarruk, J.G., Passos Dos Santos, R., Gaestel, M., David, S., 2014. TNF and increased intracellular iron alter macrophage polarization to a detrimental M1 phenotype in the injured spinal cord. Neuron 83, 1098–1116.

Liu, J., Jiang, M., Deng, S., Lu, J., Huang, H., Zhang, Y., et al., 2018a. miR-93-5p-Containing exosomes treatment attenuates acute myocardial infarction-induced myocardial damage. Mol. Ther. Nucleic Acids 11, 103–115.

Liu, J.C., Zhou, L., Wang, F., Cheng, Z.Q., Rong, C., 2018b. Osthole decreases collagen I/III contents and their ratio in TGF-beta1-overexpressed mouse cardiac fibroblasts through regulating the TGF-beta/Smad signaling pathway. Chin. J. Nat. Med. 16, 321–329.

Luo, Q., Guo, D., Liu, G., Chen, G., Hang, M., Jin, M., 2017. Exosomes from MiR-126-Overexpressing adscs are therapeutic in relieving acute myocardial ischaemic injury. Cell. Physiol. Biochem. 44, 2105–2116.

Luther, K.M., Haar, L., McGuinness, M., Wang, Y., Lynch Iv, T.L., Phan, A., et al., 2018. Exosomal miR-21a-5p mediates cardioprotection by mesenchymal stem cells. J. Mol. Cell. Cardiol. 119, 125–137.

Ma, T., Sun, J., Zhao, Z., Lei, W., Chen, Y., Wang, X., et al., 2017. A brief review: adipose-derived stem cells and their therapeutic potential in cardiovascular diseases. Stem Cell Res. Ther. 8, 124.

Mrad, M., Imbert, C., Garcia, V., Rambow, F., Therville, N., Carpentier, S., et al., 2016. Downregulation of sphingosine kinase-1 induces protective tumor immunity by promoting M1 macrophage response in melanoma. Oncotarget 7, 71873–71886.

Ohkura, S.I., Usui, S., Takashima, S.I., Takuwa, N., Yoshioka, K., Okamoto, Y., et al., 2017. Augmented sphingosine 1 phosphate receptor-1 signaling in cardiac fibroblasts induces cardiac hypertrophy and fibrosis through angiotensin II and interleukin-6. PLoS One 12, e0182329.

Saha, P., Sharma, S., Korutla, L., Datla, S.R., Shoja-Taheri, F., Mishra, R., et al., 2019. Circulating exosomes derived from transplanted progenitor cells aid the functional recovery of ischemic myocardium. Sci. Transl. Med. 11.

Sahoo, S., Losordo, D.W., 2014. Exosomes and cardiac repair after myocardial infarction. Circ. Res. 114, 333–344.

Shen, H., Wang, J., Min, J., Xi, W., Gao, Y., Yin, L., et al., 2018. Activation of TGF-beta1/alpha-SMA/Col I Profibrotic Pathway in Fibroblasts by Galectin-3 Contributes to Atrial Fibrosis in Experimental Models and Patients. Cell. Physiol. Biochem. 47, 851–863.

Shi, Y., Shi, H., Nomi, A., Lei-Lei, Z., Zhang, B., Qian, H., 2019. Mesenchymal stem cell-derived extracellular vesicles: a new impetus of promoting angiogenesis in tissue regeneration. Cytotherapy 21, 497–508.

Sica, A., Mantovani, A., 2012. Macrophage plasticity and polarization: in vivo veritas. J. Clin. Invest. 122, 787–795.

Sieve, I., Ricke-Hoch, M., Kasten, M., Battmer, K., Stapel, B., Falk, C.S., et al., 2018. A positive feedback loop between IL-1beta, LPS and NEU1 may promote atherosclerosis by enhancing a pro-inflammatory state in monocytes and macrophages. Vascul. Pharmacol. 103-105, 16–28.

Singla, D.K., 2016. Stem cells and exosomes in cardiac repair. Curr. Opin. Pharmacol. 27, 19–23.

Wu, Z., Chen, G., Zhang, J., Hua, Y., Li, J., Liu, B., et al., 2017. Treatment of myocardial infarction with gene-modified mesenchymal stem cells in a small molecular hydrogel. Sci. Rep. 7, 15826.

Yamaguchi, T., Izumi, Y., Nakamura, Y., Yamazaki, T., Shiota, M., Sano, S., et al., 2015. Repeated remote ischemic conditioning attenuates left ventricular remodeling via exosome-mediated intercellular communication on chronic heart failure after myocardial infarction. Int. J. Cardiol. 178, 239–246.

Yuan, M.J., Maghsoudi, T., Wang, T., 2016. Exosomes mediate the intercellular communication after myocardial infarction. Int. J. Med. Sci. 13, 113–116.